VARIABLE SPEED CMG CONTROL OF A DUAL-SPIN STABILIZED UNCONVENTIONAL VTOL AIR VEHICLE

K.B. Lim*, J-Y. Shin†, D.D. Moerder‡
NASA Langley Research Center
Hampton, Virginia, USA 23681

Abstract

This paper describes an approach based on using both bias momentum and multiple control moment gyros for controlling the attitude of statically unstable thrust-levitated vehicles in hover or slow translation. The stabilization approach described in this paper uses these internal angular momentum transfer devices for stability, augmented by thrust vectoring for trim and other "outer loop" control functions, including CMG stabilization/desaturation under persistent externanl disturbances. Simulation results show the feasibility of (1) improved vehicle performance beyond bias momentum assisted vector thrusting control, and (2) using control moment gyros to significantly reduce the external torque required from the vector thrusting machinery.

1 Introduction

In this paper, we focus on the vehicle controls aspect of the Vertical Take-off and Landing (VTOL) capable NASA Flying Test Platform (NFTP) as reported earlier in [1]. This earlier paper describes the recent interest in flight vehicles, capable of VTOL and hover, that are statically unstable or neutrally stable. In particular, it discusses two specific difficulties inherent in the state of the art approach to vehicle control by thrust vectoring and differential thrusting, possibly with additional aerodynamic features implemented to enhance stability in the presence of gusts. For convenience, we reiterate these concerns. First, because of the airframe's lack of stability, the controller must operate with high authority and bandwidth in order to contain and suppress excursions in attitude. Accurate system models are generally required to successfully design such controllers. The second difficulty is that such models are not available. This is because the active thrust vector variations required for stabilization in the presence of disturbances induce unsteady flow phenomena that distort the control command in a manner that is currently prohibitively difficult to model for control design. These difficulties come together when the control engineer attempts to design the required high-performance controller while ignoring or under-modelling the effect of the unsteady flow phenomena on the closed-loop dynamics. These difficulties become more evident for VTOL vehicles with smaller inertias because they respond more rapidly to disturbances so that correspondingly more rapid feedback control is necessary for vehicle stabilization.

The earlier paper [1] describes a novel approach to circumventing the problem of control-induced unsteady aerodynamics on the closed loop stability during vehicle stabilization. A tradeoff is described in which a significant level of stored bias momentum in the z-body axis provides directional stability and disturbance response mitigation at the cost of additional wheel weight and complexity of the dual spin dynamics for the system. The sizing of the bias momentum level for given nominal vehicle inertias, disturbance levels, and accuracy levels have been described. Detailed nonlinear simulations based on closed loop controlled response under strong turbulent winds and significant in-flight payload variations clearly demonstrated the significant advantages in terms of attitude and trajectory robustness.

In this paper, we demonstrate the feasibility of using a set of variable speed control moment gyros (VSCMG) to obtain controlled performance beyond what is possible through a bias momentum stability-enhanced system. We discuss a methodology for synthesis of a nonlinear controller for the system which incorporates vector thrusting and differential throttling, bias momentum wheel, and variable speed CMGs. Closed loop stability of the nonlinear system is enforced by well known Lyapunov stability conditions. Control performances are described and compared to illustrate the improvements possible through the use of CMGs, especially in its ability to reduce the commanded torque to the vector thrusting and differential thrusting machinery. The controlled performance of interest in this study is the attitude robustness of the vehicle during low airspeed or hovering operations during strong turbulent winds.

*Senior Research Engineer, Guidance and Controls Branch, kyong.b.lim@nasa.gov
†Staff Scientist, National Institute of Aerospace, j.y.shin@larc.nasa.gov
‡Senior Research Engineer, Guidance and Controls Branch, d.d.moerder@larc.nasa.gov

1.1 Outline of Paper

This paper complements the results reported recently in [1]. In the next section, a research vehicle under development at NASA Langley Research Center for maturing this control technology is described. In addition, the dynamical equations of motion about trim used specifically for control law design, and a flight dynamics and control framework are also given. Section 3 discusses controller synthesis for the system, which involves the integration of vector thrusting and CMGs for a dual spin stabilized VTOL air vehicle. A baseline set of nonlinear controllers, that can be readily designed, are described which satisfies the conditions for global asymptotic stability. In section 4, we describe simulation results that compare the performance of a set of control laws that do not use VSCMGs to a second set that do. Section 5 provides conclusions.

2 Control Design Model

2.1 NFTP Vehicle Description and Modelling Assumptions

The NFTP is designed as a laboratory-scale vehicle that is levitated by vectored thrust, additionally equipped with a suite of variable-speed CMGs and a momentum wheel that provides a substantial constant angular momentum vector aligned with the vehicle's z-body axis. A CAD model is pictured as Figure 3, and dimensional and mass properties are given in [1]. The salient features of the vehicle's dynamics are:

- mass roughly 14kg, maximum thrust roughly 200N
- principal moments of inertia roughly (.7, .7, 1.4) Kg-m^2
- z-body angular momentum bias roughly 18N-m-s
- VSCMG set output torque capacity roughly 10N-m
- peak z-axis torque due to vanes are roughly 8N-m

The net thrust vector is produced by the four ducted fans appearing in Figure 3, two of which rotate clockwise, and two counterclockwise, in order to discourage yaw torque transients related to thrust variation, and to encourage a constant value for the overall z-body angular momentum bias. Downstream from each fan is a pair of thrust-vectoring vanes. Net control force and torque vectors can be generated by differential thrusting and by deflecting the thrust vectoring vanes. These net control forces and torques are the result of adding trim control forces and torques and commanded thrust and torque deviations from trim, T_v and τ_v. For simplicity, these thrust and torque deviations are directly commanded by the control system; a numerical procedure for effiently mapping these deviations to engine and vane settings has been developed, but is not reported here. In an actual application, these required thrust and torque deviations from trim must be implemented in such a way that will account for the effects of ducted fan and motor dynamic inertial coupling with the platform to which it is attached (see [3] for details).

The momenta of the CMGs along their spin and gimbal axes are, respectively,

$$\left.\begin{array}{rcl} \dot{h}_W &=& \tau_s \\ \dot{h}_C &=& \psi + \tau_g \end{array}\right\} \tag{1}$$

where τ_s is the four-element vector of control motor torques on the wheels' spin axes, and τ_g are the corresponding control motor torques on their gimbal axes. The vector ψ contains angular momentum coupling from the platform and CMG wheel angular velocities.

Finally, the z-body location of the center of mass is near, but above the plane formed by the points at which the four fans thrust vectors are applied. Because of this, the vehicle is slightly statically unstable. Reference [1] lists a number of potential applications of vehicles of this general type. A key feature of many of them is that the center of mass of the payload is above the fan plane, and in an uncertain and variable position in the x and y-body axes.

2.2 Dynamics about trim

Trimmed flight for the NFTP, in this paper, consists of maintaining zero airframe rotation rates and translational accelerations. The CMGs, in this case, have constant spin rates and gimbal angles; thus, the CMGs take no active part in trimming the vehicle. Trim is achieved by an appropriate selection of fan speeds, $\hat{\omega}_s \in \mathcal{R}^{4\times 1}$ and vane angles, $\hat{\theta} \in \mathcal{R}^{4\times 1}$, an algorithm for which is described in [1]. Note that nonzero τ_v is generally required in order to offset gravitational torque arising from the interplay between the attitude and the center of mass location.

Denoting airframe translational and rotational velocities as v and ω, and the CMG spin axis velocity and gimbal angle vectors as Ω and η, the dynamics of the system for excursions about trim can be written as

$$\tilde{M}\dot{X} = Z + U, \quad X \triangleq \left\{\begin{array}{c} \delta v \\ \delta\omega \\ \delta\dot{\eta} \\ \delta\Omega \end{array}\right\}, \; U \triangleq \left\{\begin{array}{c} T_v \\ \tau_v \\ \tau_s \\ \tau_g \end{array}\right\} \tag{2}$$

where $\tilde{M}$ and Z are complicated nonlinear functions of the rotational states and mass properties. A detailed presentation of (2) is under preparation [3]. The form of (2) is significant, because it permits the synthesis of the Lyapunov-based nonlinear controller described in the next section.

2.3 Vehicle attitude parameterization

With the target trim attitude chosen as a reference attitude, the vehicle's attitude denoted by body frame F_b, can be conveniently viewed as an excursion about a trim frame, F_t, as shown in Figure 1. In particular, the in-

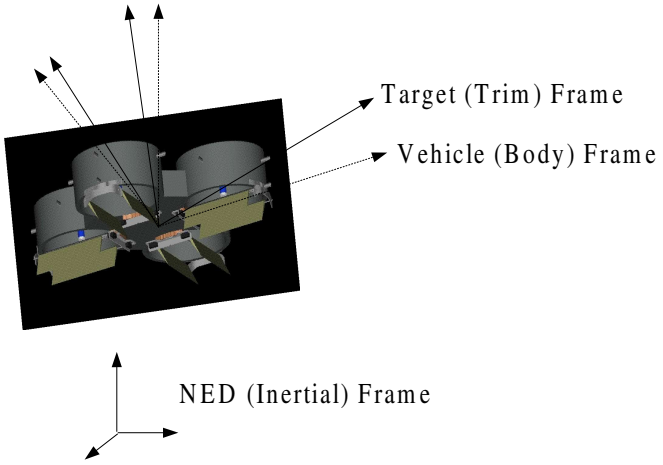

Figure 1: Reference frames for attitude tracking.

stantaneous attitude of the vehicle with respect to an inertial frame, F_o, is viewed here as a successive rotation from inertial to trim frames followed by a rotation from trim to body frame. The direction cosine matrix for the former transformation is parameterized by Euler parameters, $\hat{\beta} \in \mathcal{R}^{4\times 1}$, while the latter transformation is parameterized using Modified Rodrigues Parameter (MRP) $\epsilon \in \mathcal{R}^{3\times 1}$ [5],

$$F_t = C_{to}(\hat{\beta})F_o \quad (3)$$

$$F_b = C_{bt}(\epsilon)F_t \quad (4)$$

$$F_b = CF_o; \qquad C \triangleq C_{bt}(\epsilon)C_{to}(\hat{\beta}) \quad (5)$$

While the choice of parameterization of the directon cosine matrix for the trim frame is not crucial, it turns out that the choice of MRP to parameterize attitude deviations from trim is crucial in the generation of simple control laws with respect to attitude error feedback [6], as will be evident later. The kinematical equations governing MRP are

$$\dot{\epsilon} = \frac{1}{4}\left[(1-\epsilon^T\epsilon)I_{3\times 3} - 2\epsilon^{\times} + 2\epsilon\epsilon^T\right]\omega_{F_b/F_t} \quad (6)$$

The variable ω_{F_b/F_t} denotes the angular velocity of F_b with respect to F_t expressed in F_b frame. Hence if the trim frame does not rotate with respect to F_o then $\omega_{F_b/F_t} = \omega$, but in general, $\underrightarrow{\omega}_{F_b/F_t} = \underrightarrow{\omega} - \underrightarrow{\omega}_{F_t}$. Notice that the above MRP are directly related to the more familiar Euler parameters [5]. Unlike MRP however, the Euler Parameters are not independent but their rotational kinematics are simpler. In summary, the attitude error can be conveniently described as $\|\epsilon\|_2$, about a given trim attitude.

2.4 Control Framework

Figure 2 shows a flight dynamics and control schematic for a general NFTP vehicle with the use of both bias momentum wheel and a set of variable speed CMG's. The vector thrusting (and differential throttling) commands include four fan speeds (ω_s^{cmd}) and four vane angles (θ^{cmd}) to control platform attitude (β), and velocities (v and ω). These vector thrusting commands for the fans and vane angles are primarily used for generating trim conditions and for open loop command tracking. For the general configuration with CMGs, a secondary but nevertheless crucial function of the vector thrusting commands will be to stabilize the CMGs so that their saturation tendencies will be mitigated, as described in more detail later. To improve performance, fan speed regulators and vane servos are used.

Notice that the Ducted Fan/Vane aerodynamics and gravity directly influence system momenta p, h, while the CMG Dynamics have no influence on system momenta; rather, the CMGs internally redistribute angular momentum to control the platform angular velocity ω and its attitude β. A key advantage is that the CMG can generate internal control torques to effectively and very reliably redistribute angular momentum to control the platform, independently of Ducted Fan/Vane aerodynamics. This of course mitigates the uncertain but significant effects of unsteady aerodynamics induced by rapid control surface motions for attitude stabilization. This property of this control approach will particularly benefit smaller vehicles during hovering or operations at low airspeeds under significant wind turbulence because they will respond rapidly due to their smaller rotational inertias and will therefore require control effectors that can reliably generate control forces and moments at higher bandwidth for attitude stabilization.

While the bias momentum wheel is regulated to a certain constant speed, Ω_B, to provide directional stability in open loop, the CMG subsystem will consist of closed loop torque commands to gimbal and wheel motors for variable speed CMGs. These commands will be generated by a control law which will integrate the CMGs with the vector thrusting control system for a given momentum wheel augmented platform.

3 Controller Synthesis

An important consideration in the selection of a control law design approach in this study is global asymptotic stability (GAS) due to the inherent complexity in the nonlinear, multibody, dynamical system. In addition, the large excursions in the gimbal angles, significant gyroscopic coupling, and large attitude angle motions limits the reliability of system stability, analysis, and design methods for linear control systems. This is of particular concern when the vehicle needs to cope with strong

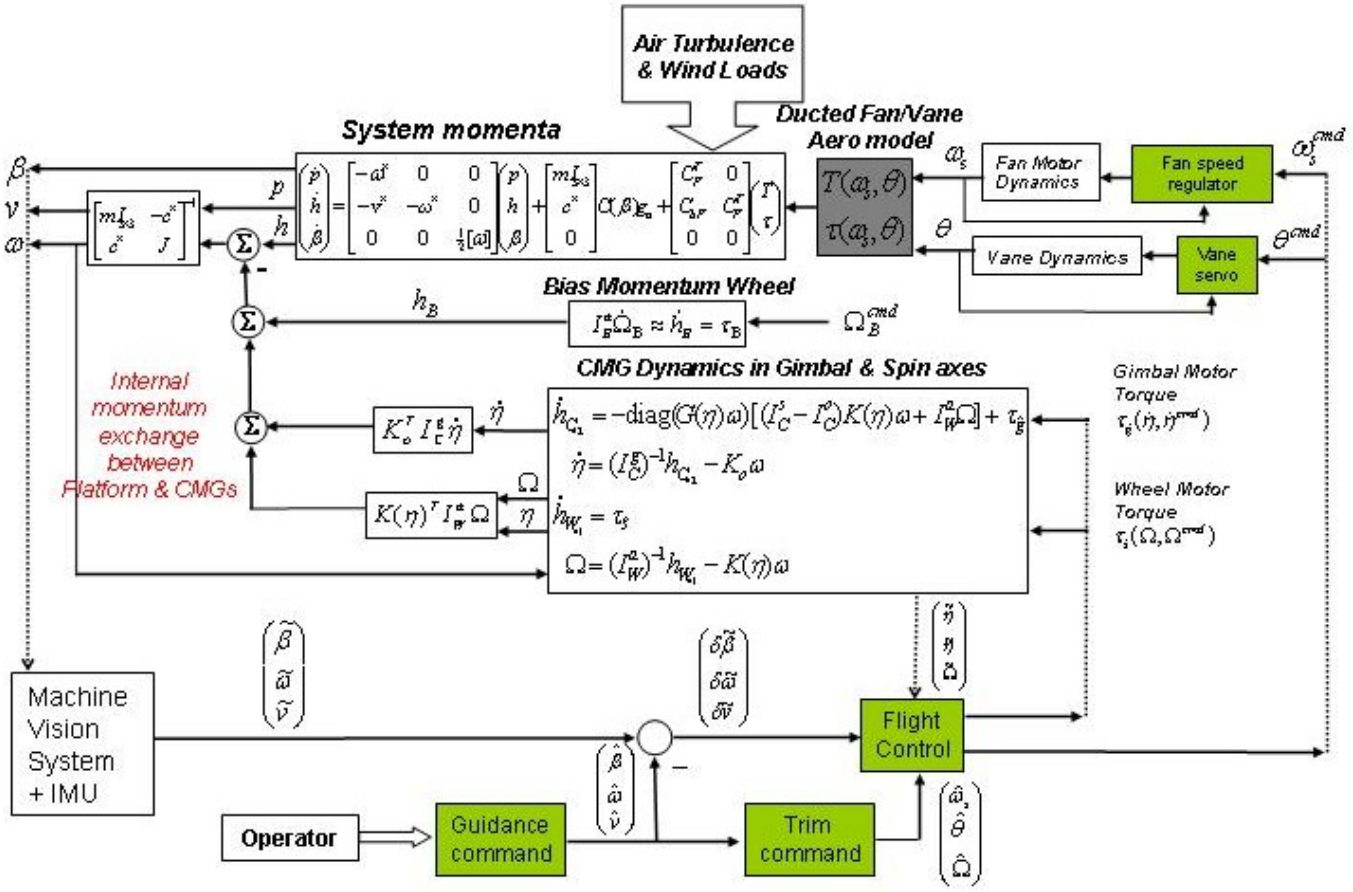

Figure 2: Flight dynamics and control schematic.

turbulent winds while hovering or flight at low airspeeds, typical of VTOL flight operations. For these reasons, we consider using Lyapunov's direct method in the control law synthesis to satisfy GAS. However, in practice even guaranteeing GAS is only a necessary condition for a successful flight since controller effectiveness and saturation can still lead to loss of vehicle. Of course in lieu of an expensive flight test program, this dilemma can be addressed, with some confidence, only through extensive simulations based on specific detailed flight hardware, for specific flight environments.

In this paper, we formulate our control problem along the lines of [6], [7], [5], and [8]. In particular, we take advantage of the control law simplifications through the use of MRP to parameterize the attitude excursions about trim, and using the particular form of the excursion error as suggested in [6]. For the CMG portion of the controller, wheel and gimbal torques are commanded, rather than the CMG output torques. In proceeding this way, we follow the approach in [9], whereby the CMG dynamics appear explicitly in the control law design. In doing so, we avoid separate vehicle control and CMG steering laws; instead, the joint control law continuously keeps the CMGs desaturated while stabilizing the airframe. This continuous desaturation is important, because a vehicle of this type operates in an environment of pervasive and unpredictable disturbances from atmospheric, manuever, and other causes, and cannot safely anticipate opportunities for dedicated "momentum dumping" events of the type typically seen when using CMGs in spacecraft control.

Define the normalized state variables

$$Y \triangleq D^{-1}X \tag{7}$$

where $Y \in \mathcal{R}^{14\times 1}$, and a normalizing non-singular diagonal matrix is given by

$$D \triangleq \mathrm{diag}(v_n, \omega_n, \dot{\eta}_n, \Omega_n) \tag{8}$$

Consider the following Lyapunov function

$$\mathcal{V} \triangleq \frac{1}{2}Y^T W Y + 2k_o \ln(1+\epsilon^T\epsilon) \tag{9}$$

where $k_o > 0$ is a scalar weight specifying the importance of vehicle attitude excursions relative to the remaining state variables, and $\{W = W^T \in \mathcal{R}^{14\times 14}, W > 0\}$ is a symmetric positive definite matrix which defines the significance of individual normalized states in the control problem. Using the motion equations in 2 and vehicle

attitude kinematics in 6, after some algebra, we can show that

$$\dot{\mathcal{V}} = Y^T \left\{ W(\tilde{M}D)^{-1}(Z+U) + D \begin{pmatrix} 0_{3\times 1} \\ k_o\epsilon \\ 0_{4\times 1} \\ 0_{4\times 1} \end{pmatrix} \right\} \quad (10)$$

One simple approach to enforce Lyapunov stability condition on the closed loop system is to choose the control input $U \in \mathcal{R}^{14\times 1}$ such that

$$\dot{\mathcal{V}} = -Y^T P Y, \quad P = P^T > 0 \quad (11)$$

which requires the following nonlinear state feedback control

$$U = -\tilde{M}DW^{-1}[PY + D \begin{pmatrix} 0_{3\times 1} \\ k_o\epsilon \\ 0_{4\times 1} \\ 0_{4\times 1} \end{pmatrix}] - Z \quad (12)$$

The weight matrix $P \in \mathcal{R}^{14\times 14}$ can be used as a matrix of control gain knobs to optimize during the controller design iterations.

Finally, note from condition 11 that only Lyapunov stability is guaranteed since the important state ϵ need not be zero for $\dot{\mathcal{V}}$ to vanish. So we state the following result that guarantees GAS.

Theorem 1 *The solution $X = 0$, $\epsilon = 0$, of the closed loop system given in equations 2, 6, and 12 is GAS.*

The significance of the above zero solution is that it corresponds to our trim solution.

Proof of Theorem 1 *We use an extension of Lyapunov stability theorem found in page 509 of [2]. It says that the system is asymptotically stable if there exists a $\mathcal{V} > 0$ such that $\dot{\mathcal{V}} \leq 0$ and such that there is no non-trivial solution such that $\dot{\mathcal{V}} = 0$.*

From the choice of $\mathcal{V}$ in 9, $\mathcal{V} > 0$, and from equation 11, $\dot{\mathcal{V}} \leq 0$. It is also clear that $\dot{\mathcal{V}} = 0$ if and only if $Y = 0$. So, what remains is to prove that the set of all solutions which also satisfies $\dot{\mathcal{V}} = 0$ consists of the null solution.

From equation of motion 2, any solution requiring $Y = 0$ means that

$$Z + U = 0 \quad (13)$$

since D is a constant, nonsingular matrix. It also follows from the feedback equation 12 that

$$U = -\tilde{M}DW^{-1}D \begin{pmatrix} 0 \\ k_o\epsilon \\ 0 \\ 0 \end{pmatrix} - Z \quad (14)$$

so that if we substitute 14 into 13, the solution variable ϵ must satisfy

$$\tilde{M}DW^{-1}D \begin{pmatrix} 0 \\ k_o\epsilon \\ 0 \\ 0 \end{pmatrix} = L\epsilon = 0_{14\times 1} \quad (15)$$

where $L \in \mathcal{R}^{14\times 3}$ is a full rank matrix since $\tilde{M}DW^{-1}D \in \mathcal{R}^{14\times 14}$ is also a full rank matrix. The only solution then is $\epsilon = 0$. The asymptotic stability applies globally since the above proof applies independent of initial conditions.

4 Simulation Results

The attitude control approach described earlier is applied to the vehicle pictured in Figure 3. More details of the test vehicle are described in the earlier companion paper [1]. The simulations presented below show that globally

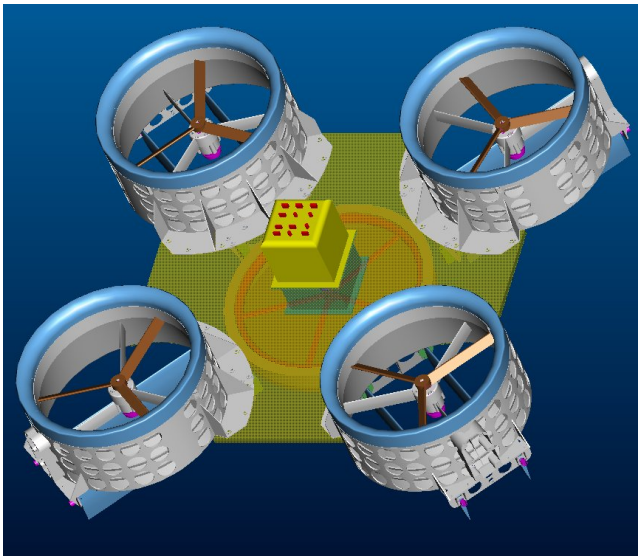

Figure 3: The NASA Flying Test Platform.

stabilizing nonlinear control laws can be developed which are capable of integrating thrust vectoring, bias momentum wheel, and active use of variable speed CMGs. In particular, the controlled performance possible beyond bias momentum stabilized system is improved by the use of a set of variable speed CMGs, analogous to the case of advanced spacecraft control systems in use today.

In our earlier paper [1], we demonstrated the fact that a system with significant level of bias momentum to provide directional stability is significantly more robust than a corresponding system with no bias momentum. So, in all simulation cases which follow, a significant level of bias momentum is assumed. Two sets of control designs are compared. The first set consist of controllers that use only vanes and fan speeds for active control. The second set uses variable speed CMGs in addition to vanes and fan speeds for active control.

4.1 Crosswind and turbulence model

To simulate wind disturbances during hovering or low airspeed operations, crosswinds are assumed which impinge on a vertical cylinder attached to the upper part of the

platform. The resulting aerodynamic drag on this cylindrical column is used to simulate the crosswind and turbulence on the vehicle. The resulting disturbance model consists of forces and torques in the pitch and roll axis. The "strong" winds are intended to simulate "Calm to Strong Breeze/Near Gale" and its simulated sample mean wind speed is 15 Knots with a standard deviation of 18, as seen in Figure 4.

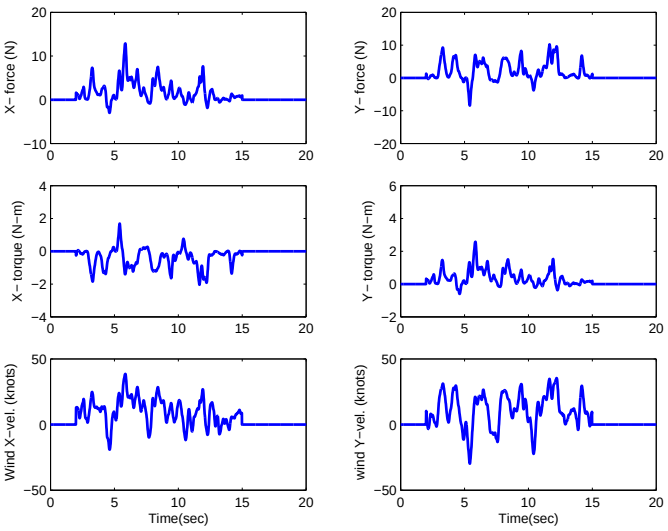

Figure 4: Simulated strong wind.

4.2 Controller Law Synthesis

Based on the control law described earlier, controllers are designed to stabilize and hold the platform attitude under strong turbulent crosswinds as described previously. For a fixed set of performance weights, W, k_o, a set of 100 randomly chosen symmetric, positive definite gain matrices, $P_{14\times14}$ and $P_{6\times6}$ are used in a closed loop simulation. Only the root mean square (RMS) values corresponding to the top 10 cases in terms of requiring the least amount of RMS torque from vector thrusting system are shown in the following figures. Hence, the control performance discussed below is only a small sample of what is possible, let alone optimal control.

Figure 5 shows the tradeoff between the RMS attitude error and the RMS torque command to the vector thrusting/differential thrusting system. This figure shows that the performance of systems using CMGs can vary widely (if carefully designed at random!) but there exists a significant set of controllers using CMGs that requires significantly less torque command to the vector thrusting system. Figures 6 and 7 demonstrate the same result except in terms of RMS thrust command to vector thrusting and RMS angular velocities.

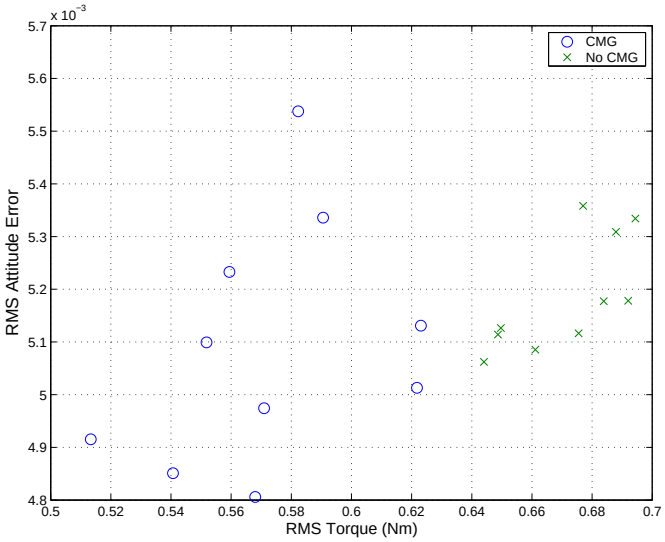

Figure 5: Attitude Response vs. Torque Command for thrust vectoring.

4.3 Minimum torque controller

Figures 8 and 9 show vehicle response comparisons for two cases. In both cases, they represent the minumum RMS torque (command to the vector thrusting system) configrations, first case (solid line) respresents the no CMG configuration, and second case (dashed line) with CMGs. These two cases corresponds to the best control gains in figure 5. Figures 8 compares the vehicle response under strong turbulent winds. The vehicle attitude excursions about trim (shown in the bottom right subplot as ϵ) is in terms of MRPs and shows robustness in the attitude response. Nice exponential decay is shown for both cases when the strong winds disappear at the end of 10 seconds. The excursions in the gimbal angle rates and CMG wheel speeds are very reasonable. Figure 9 compares the external net thrust and torque commands to the thrust vectoring system (shown as the two subplots on the top figure). These are command signals beyond trim for stabilization. Notice that the CMG case (dashed line) requires significantly less torque commands to the thrust vectoring system than the system without CMGs (solid line). The figure also shows a reasonable level of CMG wheel and gimbal motor torque commands.

5 Conclusions

This paper has examined the use of internal angular momentum transfer devices – bias momentum wheel and variable-speed CMGs, to enhance stabilization of a thrust-levitated VTOL vehicle. A nonlinear control law was formulated that satisfies conditions guaranteeing global asymptotic stability, and gains we designed via random selection. Nonlinear simulation showed significant enhancement of closed-loop attitude performance in

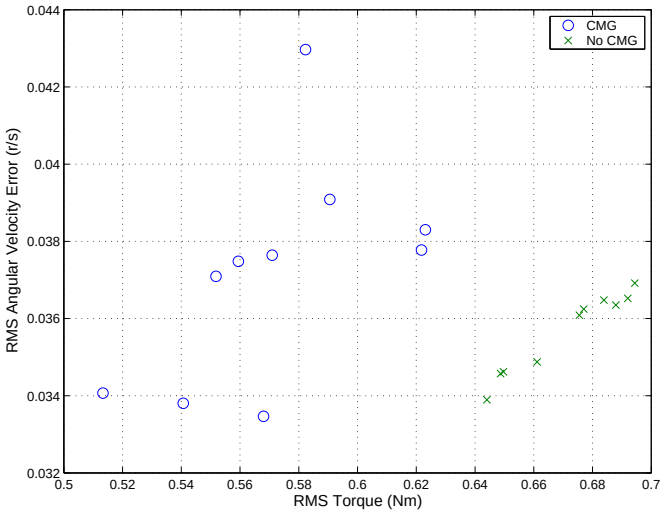

Figure 6: Angular Velocity Response vs. Torque Command for thrust vectoring.

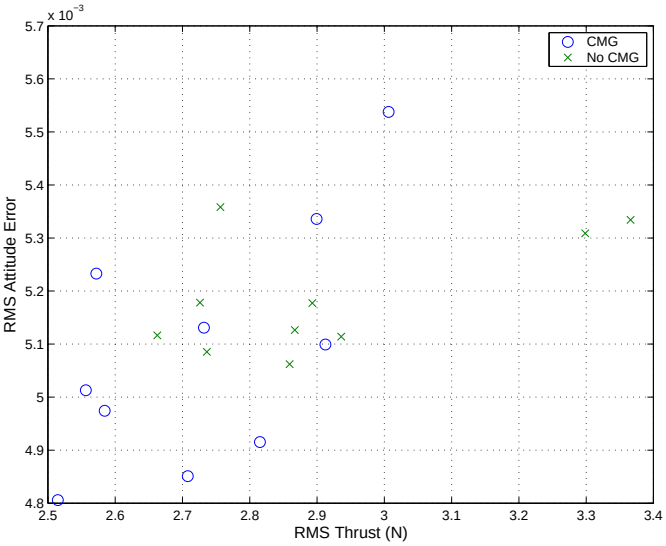

Figure 7: Attitude Response vs. Thrust Command for thrust vectoring.

hovering when subjected to cross-winds disturbances. It was also seen that the CMGs could reduce the amount of thrust vectoring actually needed for stabilization. Future work will concentrate on techniques for efficient controller design, and on formal criteria for sizing the CMGs and bias momentum against the thrust vectoring capability for this class of vehicle.

Acknowledgements

The authors would like to thank their colleagues Elvin Ahl for developing and providing the CAD figure of ongoing NFTP test configuration, and P. W. (Mike) Goode for proof reading this paper and giving tangible moral support for this research.

References

[1] Lim,K.B., Shin,J.Y., Cooper, E.G., and Moerder, D.D., "A new approach to attitude stability and control for low airspeed vehicles", AIAA Guidance, Navigation, and Control Conference and Exhibit, August 16-19, 2004, Providence, RI. AIAA Paper 2004-5008.

[2] Hughes, P.C., *Spacecraft Attitude Dynamics*, John Wiley & Sons, New York, 1986.

[3] NASA Technical Paper, to appear.

[4] Junkins, J.L., and Turner, J.D., *Optimal Spacecraft Rotational Maneuvers*, Elsevier Science Publishers, Amsterdam, Netherlands, 1986.

[5] Junkins, J.L., "Adventures on the Interface of Dynamics and Control," *Theodore von Karman Lecture*, AIAA Aerospace Sciences Meeting, Reno, Nevada, January 1997.

[6] Tsiotras, P., "New Control Laws for the Attitude Stabilization of Rigid Bodies," *IFAC Symposium on Automatic Control in Aerospace*, Palo Alto, CA, Sep 12-16, 1994, pp. 316-321.

[7] Tsiotras, P., "Stabilization and Optimality Results for the Attitude Control Problem," *Journal of Guidance, Control, and Dynamics*, Vol. 19, No. 4, 1996, pp. 772-9.

[8] Schaub,H., Vadali,S.R., and Junkins,J.L., "Feedback control law for variable speed control moment gyros," *Journal of the Astronautical Sciences*, Vol. 46, No. 3, July-Sept. 1998, pp. 307-328.

[9] Wie, B., *Spacecraft Vehicle Dynamics and Control*, 1998, AIAA Education Series, AIAA Inc., Reston, Virginia.

[10] *Spacecraft Attitude Determination and Control*, Ed. J.R. Wertz, Kluwer Academic Publishing, Boston, MA, v.73, 1995 (reprint).

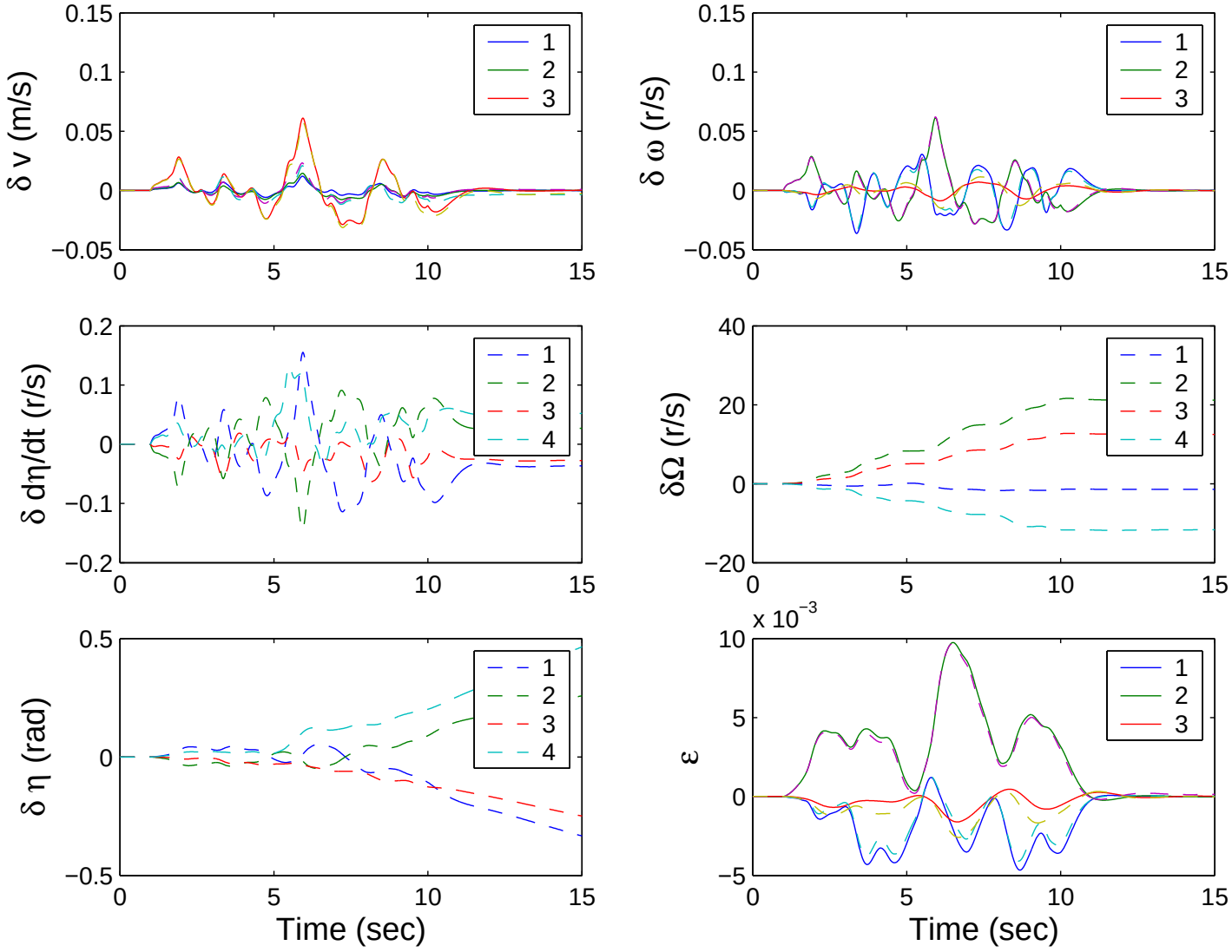

Figure 8: Vehicle response to strong wind, CMG (dash), No CMG (solid).

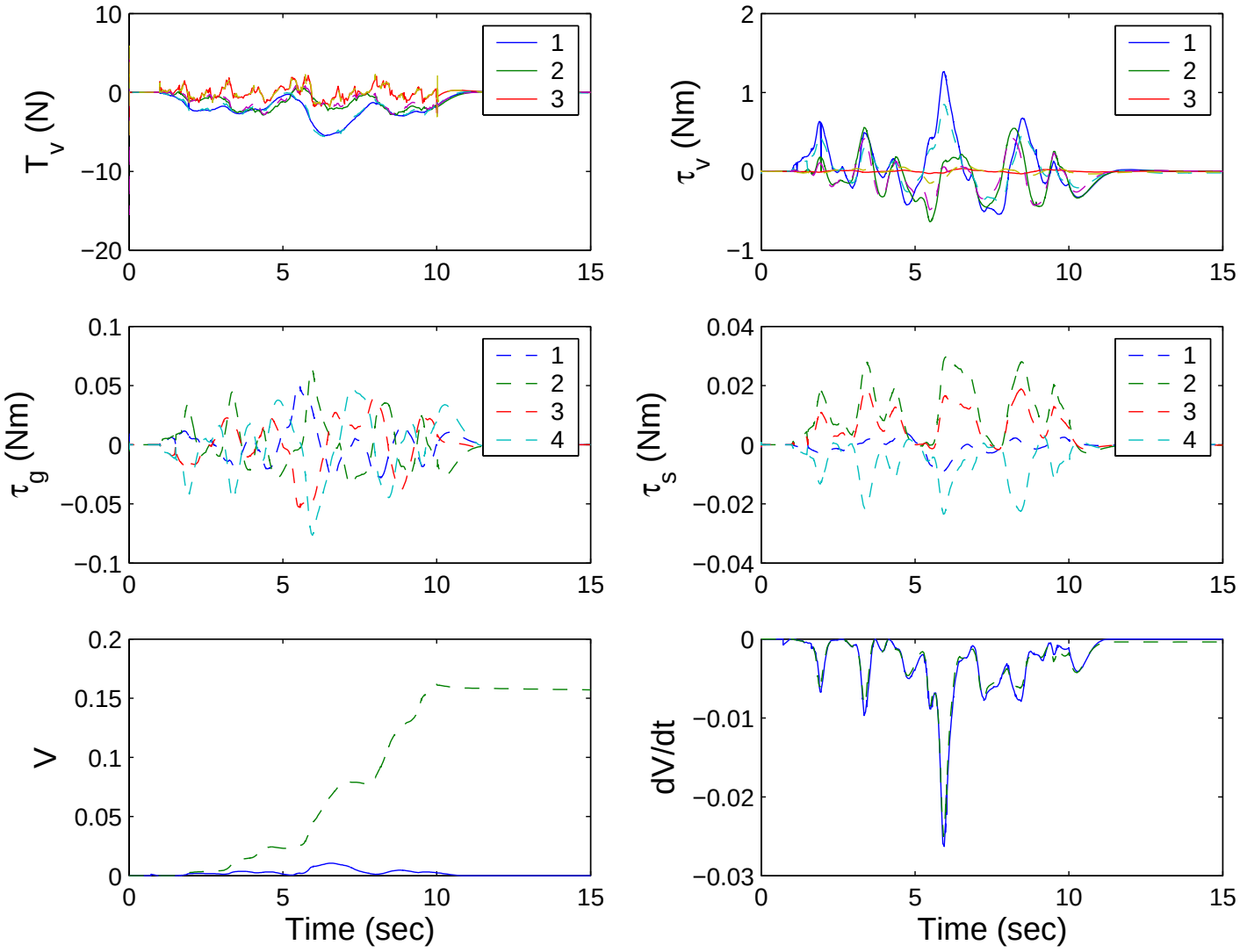

Figure 9: Control response to strong wind, CMG (dash), No CMG (solid).